TWENTY-SECOND INTERNATIONAL CONFERENCE ON COMPOSITE MATERIALS (ICCM22)

THE INFLUENCE OF GEOMETRIC IMPERFECTIONS OF DIFFERENT TOLERANCE LEVELS ON THE BUCKLING LOAD OF UNSTIFFENED CFRP CYLINDRICAL SHELLS

Tobias S. Hartwich[1] and Dieter Krause[2]
[1] Institute of Product Development and Mechanical Engineering Design, Hamburg University of Technology, Hamburg, Germany, tobias.hartwich@tuhh.de, https://www.tuhh.de/alt/pkt/home.html
[2] Institute of Product Development and Mechanical Engineering Design, Hamburg University of Technology, Hamburg, Germany, krause@tuhh.de, https://www.tuhh.de/alt/pkt/home.html

Keywords: Geometric Imperfection, Composite Shells, Buckling

ABSTRACT

Unstiffened CFRP cylindrical shells under axial compression prone to buckle. For designing these shells a high discrepancy between the theoretical analytical and the real buckling load has to be handled. Responsible for this discrepancy are various imperfections, which influence the buckling load. One of the most important and historically first considered imperfections are the geometric or traditional imperfections, which describe the deviation from the ideal form. The extent of the geometric imperfections is largely determined by the manufacture of the cylindrical shells and the boundary conditions. The fact that these imperfections are not exactly known before manufacture makes the design difficult. Therefore, despite a multitude of already existing experiments with CFRP cylinders, knockdown factors are used for the design, which lead to very conservative designs. Therefore, the statistical data base has to be extended and imperfections have to be characterized. In this paper, geometric imperfections of eleven already tested CFRP cylinders are analysed and characterised. In addition, the influence of the clamping on the geometric imperfections is investigated. Furthermore, tolerance classes are defined based on the shape tolerances that occur. Artificial cylinders are generated for the individual tolerance classes and their buckling load is calculated. Before this, a study is carried out to determine how many Fourier coefficients are necessary to describe the cylinders and how the individual modes influence the buckling load. It is shown that a reduction of the geometric imperfections increases the buckling load slightly, but decreases it significantly if the existing geometric imperfections are increased. This is particularly caused by the increase in short-wave axial imperfection modes. Finally, the geometric imperfections of another newly manufactured cylinder are analysed and characterized. This cylinder is tested on the hexapod test rig of the Hamburg University of Technology and the test results are compared with the simulation results.

1 INTRODUCTION

Thin and unstiffened cylindrical shells are a commonly used part in aerospace engineering. Two recent examples are the interstage of the Falcon 9 from SpaceX [1] and the Electron from Rocket Lab whose structure is made of carbon fibre reinforced plastic [2]. Because of this application, there are high weight and safety requirements for theses shells. Due to high radius-thickness ratios (R/t-ratio), these structures prone to buckle under axial load. However, for designing cylindrical shells, a significant discrepancy between the theoretical, analytical buckling load and the real buckling load have to be handled. Responsible for this discrepancy are various imperfections, like geometric imperfection, load imperfection and other disturbances like scattering of material parameter. To consider these imperfections the NASA SP-8007 was developed in the 1960s to design reliable cylindrical shells. It suggests knockdown factors based on test of metallic cylinders under various boundary conditions [3]. However, this guideline leads to conservative designs for cylindrical shells made of composite materials [4]. Therefore, new design guidelines have to be developed and all relevant influence factors have to be characterized. The aim of this paper is to analyse the influence of geometric imperfections of different tolerance classes on the buckling load in order to support the development of new design guidelines.

2 DESIGN OF THIN-WALLED CFRP CYLINDER SHELLS

The design of thin-walled cylindrical shells under axial compressional loads has been the subject of research for more than one hundred years. First solutions for the determination of the buckling load were presented by Lorenz [5], Timoshenko [6] and Southwell [7] at the beginning of the 20th century. Experiments during the next decades showed significantly lower experimental buckling loads compared to predicted ones. In 1934 Donnel developed an approach for the design of thin-walled cylinders under compression and bending stress based on his own and external tests, which also take into account large displacements and imperfections in the form of a double harmonic series [8]. In his dissertation in 1945 Koiter describes the close connection between geometric deviation from a perfect cylinder and the observed reduced buckling load. This work received more attention when it was translated into English in 1970. Koiter considers geometric imperfections in the form of double Fourier series and shows that the imperfection pattern is important for the estimation of a knockdown factor [9].
The currently still valid design guideline is the NASA SP 8007 which proposes a knockdown factor depending on the R/t-ratio. This is based on a large number of tests with metallic cylinders from the 1930s to 1960s [3]. However, in these experiments typical specific parameters of CFRP are not considered. Therefore, this guideline leads to relative conservative designs for cylindrical shells made of CFRP [4]. Another design method is the Single Perturbation Load Approach proposed by Hühne, which delivers higher buckling loads than NASA SP 8007 [10]. However, it provides in some constellations higher loads than experimentally demonstrated [11]. Since any imperfections are random, the use of probabilistic methods is appropriate to take them into account of the design process. The first approaches have been available since the early 1960s, such as the one developed by Bolotin [12]. The probabilistic approaches have been further developed over the past 60 years, but because of the insufficient statistical database the use of these approaches without assumptions remains critical.

3 THE INFLUENCE OF GEOMETRIC IMPERFECTIONS

As shown in the previous chapter, some of the most relevant impact factors on the buckling load are the geometric imperfections or so-called traditional imperfections. Apart from the manufacture, the boundary conditions, like the clamping of the cylinder, influence the geometric imperfections.

3.1 Definition and Description of Geometric Imperfections

Geometric imperfections are deviations of the ideal form and most common described by Fourier coefficients. In contrast to metallic cylinders, CFRP cylinders tend to have longer wavelength imperfection patterns due to the manufacturing process [13]. In literature there are two common approaches to model the imperfections [14]. One is the half wave cosine and the other is the half wave sine approach. Since the half wave sine approach has always a trivial solution ($\sin(k\pi x/L) = 0 \; for \; x = 0, L$) at the ends of the cylinders, the half wave cosine is used in this paper to include geometric imperfections at the ends of the cylinders.

$$\bar{W}(x,y) = 2t \sum_{k=0}^{m} \sum_{l=0}^{n} \cos\frac{k\pi x}{L} \left(A_{kl} \cdot \cos\frac{ly}{R} + B_{kl} \cdot \sin\frac{ly}{R} \right) \tag{1}$$

The variables A_{kl} and B_{kl} are the Fourier coefficients. L describes the cylinder's length, R is the radius and t is the wall thickness of the cylinder. The indices k and l indicate the number of half waves in the axial direction and the number of full waves in the circumferential direction. Describing geometric imperfections in the Fourier coefficients as shown here is partly due to the fact that imperfection patterns are stored in this form in the international imperfection database in Delf and Haifa, thus enabling a comparison of different imperfections [15].

3.2 The Influence of the Clamping

For the testing of the cylinders, a connection between the cylinder and the test rig has to be realized. In general, there are two possibilities to realize this connection. One possibility is to clamp the cylinders, the other one is to glue them freely glued into the connection, for example into a groove. To reduce the geometric imperfections the cylinders are mounted in a clamped solution, which is described in [16]. With the reduction of the geometric imperfection through clamping the cylinder the buckling load increases like it is shown on epoxy cylinders in [17].

In Figure 1 the reduction of the geometric imperfections through the clamping is shown by a winding-up of a cylinder surface before and after clamping. However, calculating the Fourier coefficients shows that the clamping only reduces the longer modes. Nevertheless, simulations indicate that these radial modes with two full-waves have only a small impact on the buckling load, although these modes have relative high amplitudes.

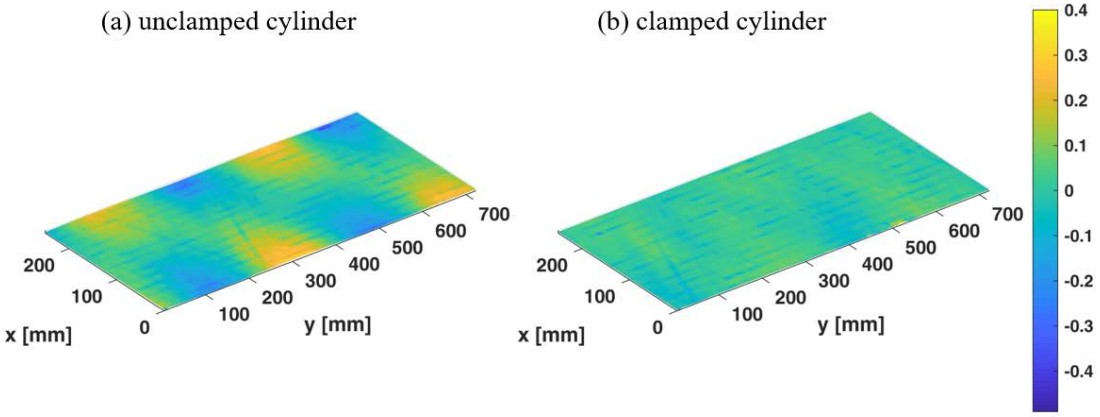

Figure 1: Winding-up of a cylinder surface before (a) and after (b) clamping.

4 ANALYZING DIFFERENT TOLERANCE LEVELS OF GEOMETRIC IMPERFECTIONS

In this chapter the geometric imperfections of eleven CFRP cylinders are analysed. Based on these geometric imperfections tolerance classes are defined. New artificial cylinders are generated for each tolerance class and the referring buckling loads are calculated.

4.1 Characterization of the Existing Cylinders

The cylinders are manufactured in a filament winding process at the DLR Braunschweig. The cylinders' material is an AS7 fibre with an 8552 matrix. The cylinders have a nominal layup of $[90°/30°/-30°]_S$. However, due to the manufacturing processes the layup of 30°-layers varies over the cylinder. The nominal length is 215 mm, nominal radius is 115 mm and the nominal thickness is 0.81 mm [3].

In a first step the range of the geometric imperfection of these cylinders is determined. The range of the cylinders' deviation of the ideal geometry lays between 0.20 mm and 0.09 mm on the upper end and between -0.19 mm and - 0.01 mm on the lower end. The mean is 0,14 mm or respectively -0.11 mm. Compared to other tested cylinders, like shown in [10] and [4], the cylinders are relatively thick and the maximum amplitudes are relatively small. For further information on the cylinders, such as the calculated Fourier coefficient, refer to [18].

4.2 Modelling of the Cylinders

The cylinders are modelled with S4R shell elements in AQAQUS/implicit. Based on the convergence study by [16] a mesh size of 214 x722 elements is chosen. To take the geometric imperfections into account, the data recorded by the ATOS system is further processed in Matlab and the imperfections are

mapped into the model nodes via the calculation and use of the Fourier coefficients. With the ATOS measurement results a geometric mesh is calculated in a proprietary software of the company of the measurement system. Based on this geometric mesh, measuring points are chosen in a selected resolution for further processing.

At first, the necessary resolution of the measured geometry is determined. For this purpose, the calculated Fourier coefficients of different resolutions of the measured geometry are compared pairwise. Results show that there is no relevant difference to higher resolutions in the examined cylinders with a resolution of 51 x 174 measuring points. In a second step a study to determine the number of relevant Fourier coefficient is carried out. The possible number of Fourier coefficients is limited by the resolution of the geometry data of the ATOS measurement. The number of axial and circumferential Fourier coefficients is gradually increased and the buckling load is calculated and compared with the experimental load. It turns out that the calculated buckling load is lower than the experimental load when many Fourier coefficients are taken into account. The reason for this may be the consideration of peel ply textures, which have relatively short wavelength patter but do not influence the relevant geometry for the buckling load. However, when fewer Fourier coefficients are used the buckling load is overestimated. Furthermore, the optimum number of Fourier coefficients varies between the cylinders. Nevertheless, 15 coefficients in axial direction and 12 coefficients in circumferential direction have proved to be practicable for all cylinders.

4.3 Varying the Geometric Imperfection

Based on the existing geometric imperfection, five different tolerance classes of geometric imperfections are as follows defined. Two smaller and two wider tolerance classes are chosen around the tolerance class T2 (see Fig. 2), in which all existing cylinders are arranged. The maximal value of the amplitudes is doubled between every tolerance class. To evaluate these classes new artificial cylinders are generated based on the distribution of the Fourier coefficients of the existing ones.

$$A_{i,j} = \lambda\left(A_{i,j,mean} + A_{i,j,std} \cdot randn\right) \tag{2}$$

The function *randn* generates a randomly normally distributed number between zero and one. The scalars $A_{i,j,mean}$ and $A_{i,j,std}$ are the mean and the standard deviation of each Fourier coefficient of the analysed cylinder set. Whereas λ scales the generated Fourier coefficient for each tolerance class. With this approach imperfection pattern are generated, which are very similar to the existing ones.

The buckling load of the generated cylinders is calculated. Since lateral forces occurred in the considered experiments, the mean value of the occurring lateral forces ($F_x = -1.23\ kN; F_y = 2.70\ kN$) is assumed for the calculations of the buckling loads of the artificially generated cylinders in order to receive realistic buckling loads. However, with the use of a mean value of occurring lateral forces there is no influence of the scattering of the lateral forces on the scattering of the buckling load. Table 1 lists the maximum imperfections considered for the tolerance class, the calculated mean buckling load and their scatter. In Figure 2 the scattering of the buckling load of each tolerance class is depicted.

Tolerance class	Tolerance range [mm]	Average buckling load [kN]	Standard deviation buckling load [kN]
T0	$\pm$ 0.05	62.22	0.12
T1	$\pm$ 0.10	61.81	0.28
T2	$\pm$ **0.20**	**60.36**	**0.67**
T3	$\pm$ 0.40	56.58	1.67
T4	$\pm$ 0.80	47.60	1.51

Table 1: Tolerance class and average calculated buckling load.

Higher amplitudes of the whole Fourier spectrum lead to lower buckling loads. For instance, reducing the range of the existing amplitudes (T2) by 50 % leads to 2.4 % higher buckling load and reduces the standard deviation between the cylinders by 58.2 %. Whereas, doubling the tolerance range results in a

decrease of the buckling load of 6.3 % and the scattering increases by 145 %. In contrast to the relatively high amplitude of the first low radial modes of the unclamped cylinder, an increase of the whole spectrum of imperfections leads to significant lower buckling loads.

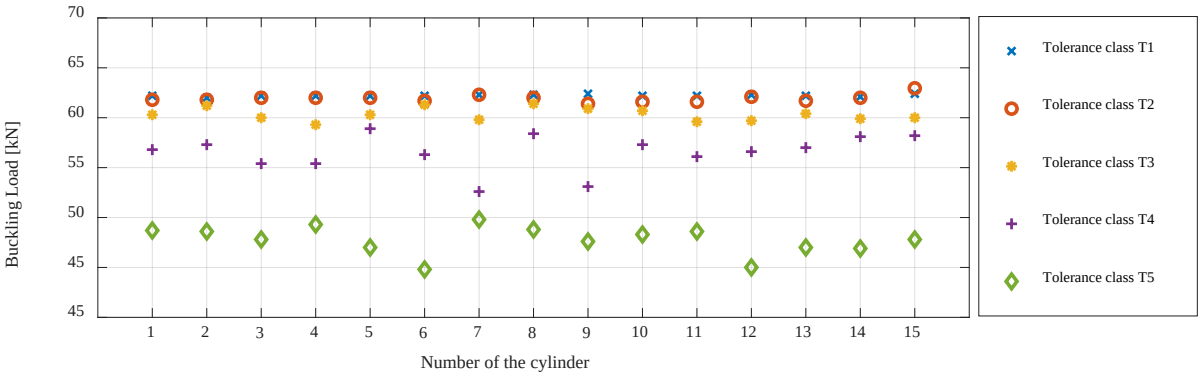

Figure 2: Scattering of the calculated buckling load of the artificial cylinders.

In a further study, individual modes are increased and the effect of increasing different modes on the buckling load analysed. The second, fourth, sixth, eighth and tenth modes of two cylinders are increased to a value of 0.5 mm in both the axial and circumferential directions. This means that these generated cylinders are in tolerance class T4, whereby they are close to tolerance class T3.

The calculated buckling load of the two arbitrary chosen cylinders considered without increasing individual modes is 59.56 kN and 60.16 kN for comparison. In Figure 3 the results of the calculation are depicted. The reduction of the buckling load as a result of the increase of individual modes behaves qualitatively and quantitatively the same way for both considered cylinders. There are basically two trends. The shorter the wavelength of a mode, the higher the reduction of the buckling load resulting from an increase in the amplitude of a mode. Furthermore, the increase of amplitudes of the modes in the axial direction leads to a significantly greater reduction of the buckling load. This can be explained since, as especially long-wave modes in circumferential direction are to be understood as ovalization, which has little influence on the buckling load.

In summary the increase of the entire mode spectrum leads to a reduction of the buckling load. Especially the higher wavelength modes in axial direction are decisive for this, whereas the amplitude of long-wave circumferential modes which, for example, are reduced by clamping have a very small influence.

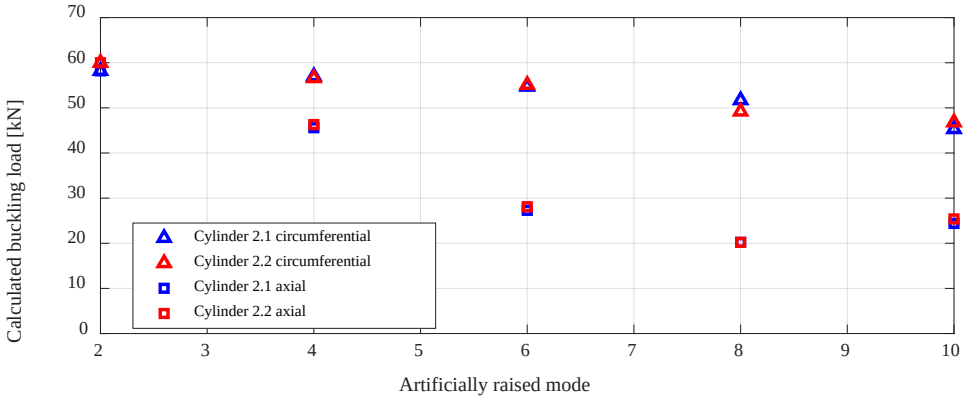

Figure 3: Scattering of the calculated buckling load of the artificial cylinders.

5 TRANSFER TO A SECOND SET OF CYLINDERS

For the further investigation of the defined tolerance classes, they must be validated by further tests. In this chapter a further cylinder is measured and tested.

5.1 Test and Test Setup

Based on these results a new set of six CRFP cylinders with similar material parameters and geometric properties are developed and manufactured by the DLR Braunschweig. Again, the geometric imperfections of the clamped cylinders are measured with ATOS system from GOM and compared with the results described earlier. Furthermore, one of these cylinders was tested on the hexapod test rig of the Hamburg University of Technology for validation.

The hexapod test rig is 6 degree of freedom (dof) movement platform which is able to execute various static and dynamic test. Further details of the test rig are described in [19]. In Figure 4 the test setup is shown. The clamped cylinder is placed on the 6 dof load cell. On the cylinder six strain gauges are placed circumferentially. Furthermore, three optical displacement sensors are used in order to track an inclination of the cylinder. For the connection between the fixture of the cylinder and the platform of the test rig two solutions as described in [18] are used. The first solution is the clamped support which connects the cylinder with test rig in all dofs. The second solution consists of a ball-and-socket-joint and introduces the load in the middle of the cylinders clamping. Therefore, inclinations are possible with the second solution.

In contrast to [16] the clamped support is chosen first because it rather corresponds to the boundary condition of the application case. After six elastic compression and tension tests the buckling test was repeated ten times with clamped support. The buckling test was then carried out with the ball-and-socket-joint connection to determine the influence of the boundary condition induced by the connection.

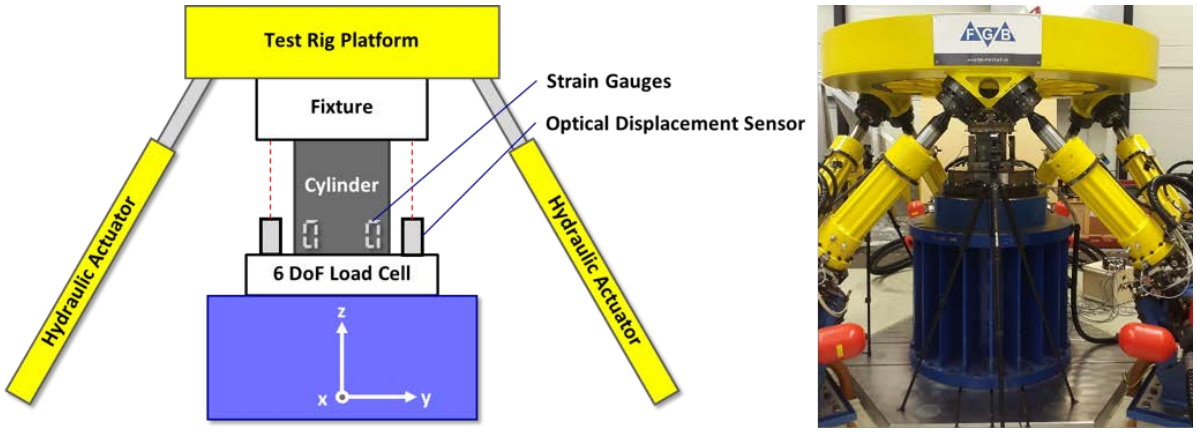

Figure 4: Test setup of buckling test on the Hexapod test rig.

5.2 Test Results

Before the buckling tests were carried out the surface of the clamped cylinder was measured by an ATOS system. The extend of the geometric imperfections are analysed. Furthermore, the Fourier coefficient are calculated and shown in Figure 5 on the left side. On the right side of Figure 5 there is a winding up of the clamped cylinder's surface. As determined in Chapter 4, 12 rotating full waves and 15 axial half waves are considered for later simulations.

The range of the cylinder's deviation of the ideal geometry lays between 0.12 mm on the upper end and -0.21 mm on the lower end. Therefore, this cylinder fits best into the tolerance class T2. However, the deviation on the upper end is very close to tolerance class T1 and the lower end is actually just within the range of tolerance class T3. But the range from the upper to the lower end is 0.33 mm which fits best to the tolerance class T2 with range 0.4 mm. Furthermore, the second and fourth circumferential full-wave are very distinct, which is consistent with the literature where CFRP cylinders tend to long wave imperfections [13], [16].

(a) Fourier coefficent of the tested cylinder

(b) windig-up of the tested cylinder

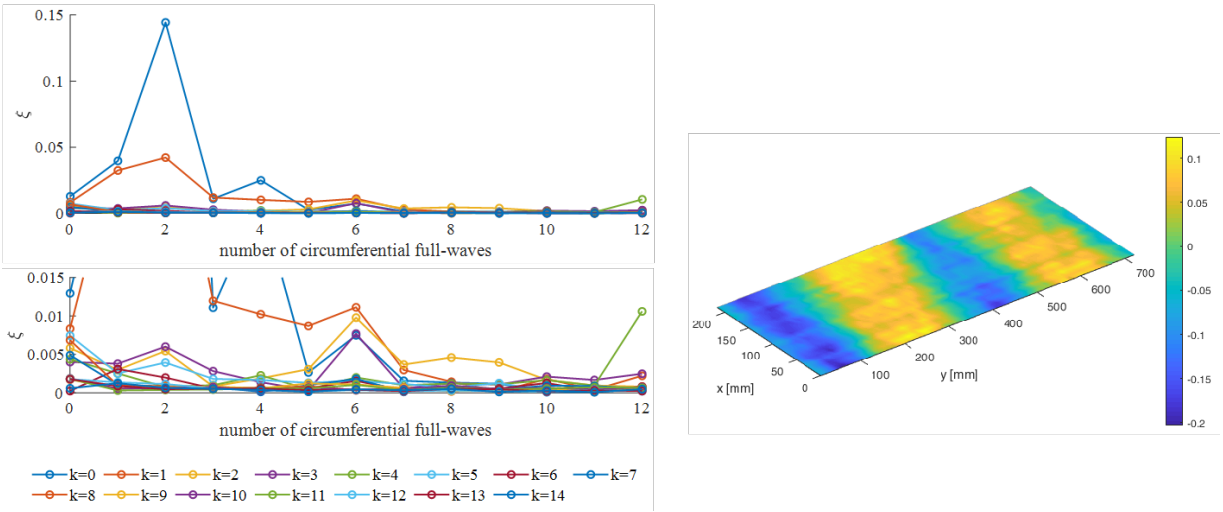

Figure 5: Fourier coefficient of the tested cylinder (a) and winding-up of a cylinder surface after clamping (b).

Ten buckling tests are carried out with the cylinder in the clamped support. In the first test a buckling load of 59.87 kN occurs. In the second test the buckling load decreases to 57.49 kN. In the third test the buckling load increases to 59.45 kN. However, the next seven tests have results between 58.60 kN and 57 kN. Even the tenth test reached a load of 57.78 kN. In the following the ball-and-socket-joint connection was used. In this test setup a buckling load of 57.78 kN was determined. After that the cylinder was destroyed during the next test. In Figure 6 the graph of the occurring axial loads of six buckling test are plotted. Five are carried out with the clamped support and one is carried out with the ball-and-socket-joint connection (simple).

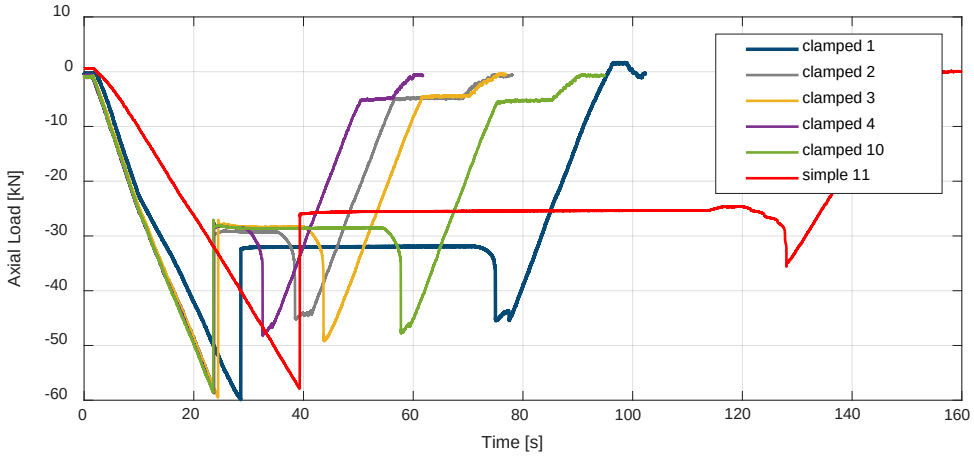

Figure 6: Course of axial compressive loads including buckling loads.

Since the buckling load only decreases marginally over the cylinder specific tests and partly increases again, an elastic buckling behaviour is assumed. However, for a prove this would require the laminate to be checked for fibre breaks and delamination. Since the cylinder was destroyed as a result of another test, this has to be checked again with another test specimen. However, the lateral forces occurring from the first to the second test change by about 0.5 kN in both the x and y directions. In all following tests with the fixed clamping, the course of the lateral forces looks the same as in the second test. This may indicate that smaller failure effects occurred as a consequence of the first test.

With a maximum buckling load of 59.87 kN and an average of 58.5 kN, this cylinder lies exactly between the buckling loads of tolerance classes T2 and T3. This means that the buckling load corresponds exactly to the range in which the cylinder was classified by the geometric imperfections. This test thus confirms the results of the defined tolerance classes. However, for a validated statement, further cylinders with the same and different radius-thickness ratio have to be tested.

Compared to the carried out test, the buckling load decreases over the number of tests carried out in Schillo [18]. The maximum buckling load of 59.87 kN, on the other hand, is within the range of the average buckling load of 59.3 kN determined by Schillo over eleven cylinders [18]. As can be seen in Figure 7, the fixed clamping leads to lower lateral forces than a simple articulated clamping as used in the last test and by Schillo [18]. When using simple clamping the occurring lateral forces are comparable in direction and magnitude to those found by Schillo [18]. One possible cause for the high lateral forces in the use of the simple clamping could be a not optimally centric force introduction. Minor inhomogeneities and subsequent tilting can increase the applied lateral forces further.

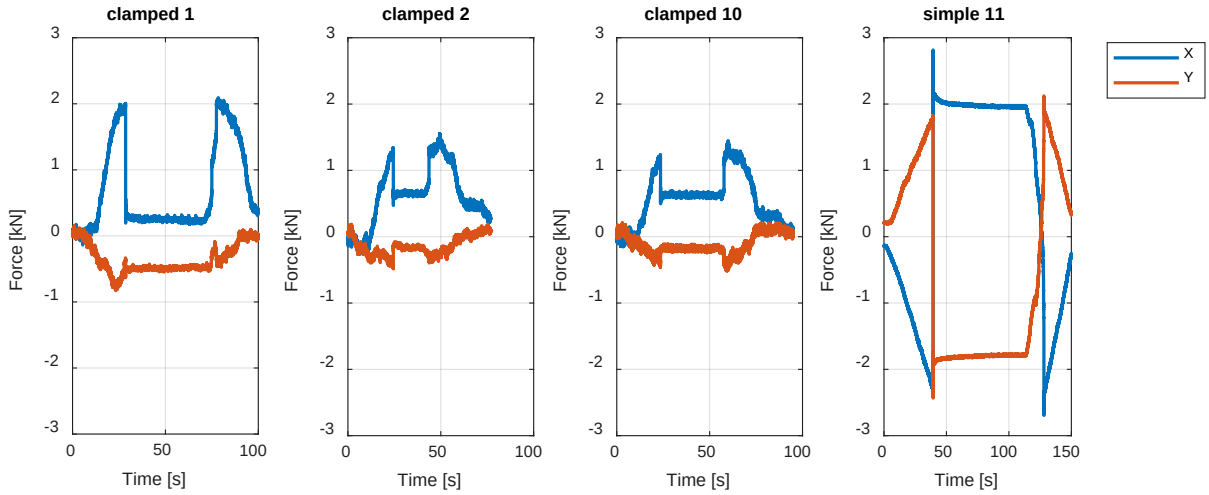

Figure 7: Occurring lateral forces.

6 CONCLUSIONS

The geometric imperfection of a set of eleven CFRP cylinders are analysed. Long-wave circumferential imperfections can be reduced by clamping the cylinders, but these imperfections have a small influence on the buckling load. In order to model the geometric imperfections of the given cylinders, 12 Fourier coefficients in the circumferential direction and 15 Fourier coefficients proved to be practicable. The evaluation of the five tolerance classes based on the eleven cylinders shows how the buckling load decreases with increasing form deviation. However, an increase in individual modes shows that long-wave circumferential modes have hardly any influence on the buckling load, which means that they have to be less considered in the definition of a manufacturing tolerance. In a further test, one of a new set of CFRP cylinder is measured and subsequently tested. The results support the defined tolerance classes. However, these results must be substantiated with further test results. Cylinders with different dimensions (R/t-ratio), layer structures and a different manufacturing process should be tested.

Furthermore, the test shows how the boundary conditions of the test setup influence the test result. In addition, there is a buckling behaviour which indicates elastic buckling. These two aspects have to be investigated further. Nevertheless, this paper proposes five suitable tolerance classes for the design of CFRP cylinders and shows how especially short-wave axial geometric imperfection influence the buckling load.

ACKNOWLEDGEMENTS

This research was funded by the German Research Foundation (DFG) via the project "Zuverlässigkeitsbasierte Auslegung unversteifter CFK-Zylinderschalen unter Material- und Strukturunsicherheiten".

REFERENCES

[1] SpaceX, Falcon 9, 2019, https://www.spacex.com/falcon9, accessed 28th May 2019.
[2] J. Tulp and P. Beck, Rocket Lab: Liberating the Small Satellite Market, in: *31st Annual AIAA/USU Conference on Small Satellites*, 2017.
[3] V.I. Weingarten, P. Seide, J.P. Peterson, *NASA SP 8007 - Buckling of thin-walled circular cylinders*, 1968.
[4] R. Degenhardt, A. Kling, A. Bethge, J. Orf, L. Kärger, R. Zimmermann, K. Rohwer and A. Calvi, Investigations on imperfection sensitivity and deduction of improved knock-down factors for unstiffened CFRP cylindrical shells, *Composite Structures*, **92**, 2010, pp.1939–1946 (doi: 10.1016/j.compstruct.2009.12.014).
[5] R. Lorenz, Achsensymmetrische Verzerrungen in dünnwandigen Hohlzylindern, *Zeitschrift des Vereins Deutscher Ingenieuere*, **52**, (1908), pp.1706–1713.
[6] P. Timoshenko, Einige Stabilitätsprobleme der Elastizitätstheorie, *Zeitschrift für angewandte mathematische Physik*, **58**, 1910, pp.353–361.
[7] R.V. Southwell, On the general theory of elastic stability, *Philosophical Transactions of the Royal Society*, **213**, 1914, pp.187–244.
[8] L.H. Donell, A new theory for the buckling of thin cylinders under axial compression and bending, *Transactions ofthe ASME*, **56**, 1934, pp.795-806.
[9] W.T. Koiter, *The stability of elastic equilibrium*, Hampton, 1970.
[10] C. Hühne, R. Rolfes, E. Breitbach and J. Teßmer, Robust design of composite cylindrical shells under axial compression — Simulation and validation, *Thin-Walled Structures*, **46**, 2008, pp.947–962 (doi: 10.1016/j.tws.2008.01.043).
[11] B. Kriegesmann, E.L. Jansen and R. Rolfes, Design of cylindrical shells using the Single Perturbation Load Approach – Potentials and application limits, *Thin-Walled Structures*, **108**, 2016, pp.369–380 (doi: 10.1016/j.tws.2016.09.005).
[12] V.V. Bolotin, *Statistical methods in the nonlinear theory of elastic shells*, Washington, 1962.
[13] M.K. Chryssanthopoulos and C. Poggi, Probabilistic imperfection sensitivity analysis of axially compressed composite cylinders, *Engineering Structures*, **17**, 1995, pp.398–406 (doi: 10.1016/0141-0296(95)00048-C).
[14] J. Arbocz and J.H. Starnes Jr., Future directions and challenges in shell stability analysis, *Thin-Walled Structures*, **40**, 2002, pp.729–754 (doi: 10.1016/S0263-8231(02)00024-1).
[15] J.d. Vries, *The imperfection data bank and its applications*, Delf University of Technology, 2019.
[16] C. Schillo, D. Röstermundt and D. Krause, Experimental and numerical study on the influence of imperfections on the buckling load of unstiffened CFRP shells, *Composite Structures*, **131**, 2015, pp.128–138 (doi: 10.1016/j.compstruct.2015.04.032).
[17] C.G. Foster, Axial compression buckling of conical and cylindrical shells, *Experimental Mechanics*, **27**, (1986), pp.255–261.

[18] C. Schillo, *Reliability based design of unstiffened fibre reinforced composite cylinders*, Hamburg University of Technology, 2016.
[19] B. Plaumann, O. Rasmussen and D. Krause, System analysis and synthesis for the dimensioning of variant lightweight cabin interior, *54th AIAA/ASME/ASCE/AHS/ASC Structures, Structural Dynamics, and Materials Conference, Boston, United States*, 2013.